7.2 DAMAGE MECHANISM INTERACTIONS AT THE PLASMA-MATERIALS INTERFACE (Early Career Award)—C. M. Parish, K. Wang (Oak Ridge National Laboratory)

OBJECTIVE

This work intends to develop the fundamental scientific basis for modelling and predicting the behavior of helium bubbles in refractory materials, to provide support for the science and engineering of the tokamak plasma-facing-material environment.

SUMMARY

This reporting period has emphasized experimental technique developments as the necessary foundation for all later work, continued collaborations with other institutions, and has begun exploration of defect-defect interactions within plasma-exposed and neutron-irradiated tungsten.

PROGRESS AND STATUS

Introduction

As the choice for the ITER divertor, and present leading candidate for subsequent tokamak systems, tungsten metal is the current focus for high-flux, high-fluence, high-temperature plasma-materials interactions (PMI) studies. Unfortunately, the fundamental scientific basis for explaining observed PMI behaviors (e.g., nanofuzz growth) and predicting long-term behaviors (e.g., PMI response in a nuclear environment) is lacking. In this reporting period, we have examined neutron-irradiated and plasma-exposed tungsten in order to begin building up the understanding and methods for quantitative characterization of defects in these materials.

Experimental Procedure

In this summary, data from several sets of experiments are presented. Transmission Kikuchi diffraction (tKD) was performed in a JEOL 6500F SEM using an EDAX EBSD system, with beam parameters of 20-30 keV, 3-5 nA. TEM and STEM imaging and microanalysis were performed at ORNL LAMDA lab using the FEI Talos F200X instrument.

Results

<u>Neutron-irradiated tungsten</u>

Eventually, in-reactor plasma-facing components (PFCs) or materials will experience high neutron loads. Developing a predictive capability for PMI behavior will require a quantitative analysis of the evolving neutron-irradiated structure. In collaboration with the ORNL PFC team, we performed STEM X-ray spectrum imaging, followed by multivariate statistical analysis (MVSA) datamining, to evaluate the structure of the neutron-irradiated polycrystalline tungsten specimens from the previous HFIR irradiation campaign. Figure 1 shows a typical dataset, in which Re-Os rich precipitates heavily penetrate a W-rich matrix. Re is seen to heavily line the irradiation-induced cavities and the grain boundaries.

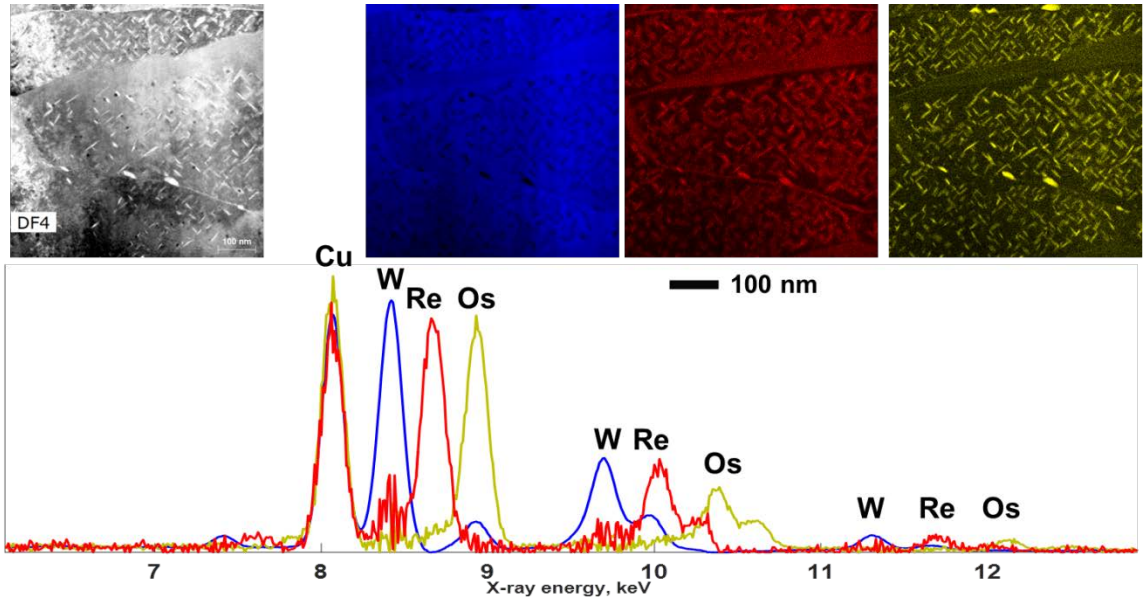

Figure 1. Medium-angle annular dark field ("DF4") image and three MVSA-derived component images. The component spectra are also shown. The W, Re, and Os components are clearly separated by datamining. Cu counts are from the sample holder. ~4 dpa, ~700°C.

Identification of the precipitates is underway. Due to highly overlapping precipitates within the foil thickness and severe irradiation damage, this is not a straightforward analysis. Figure 2 illustrates combined electron diffraction and high-resolution imaging to analyze the precipitate structures.

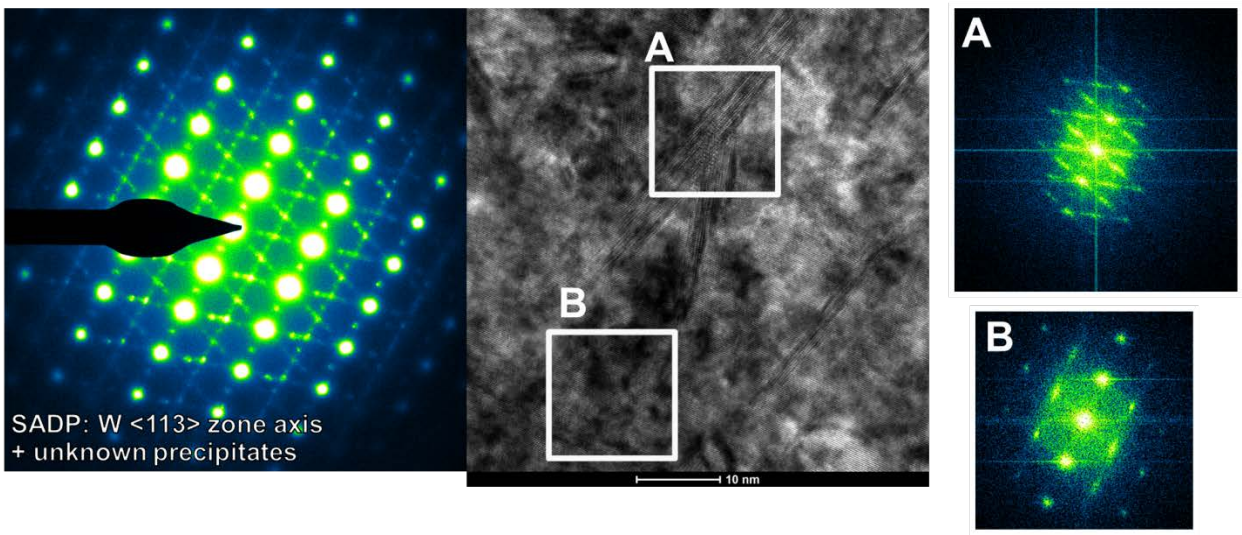

Figure 2. Electron diffraction pattern (left) and high-resolution TEM image (center). The two regions marked A and B have their Fourier transform diffractograms presented on the right. Interestingly, B appears to be matrix but shows superlattice peaks. This is under further exploration.

Several different irradiation conditions have been examined, and work is underway to quantify the microstructures.

Low-energy helium exposure of surfaces

Presently, we are addressing the question of how internal intrinsic defects (dislocations, grain boundaries, etc.) influence the disposition of helium under PMI conditions. We performed a series of helium surface exposures (80 eV, ~10^{20} He/m^{2}sec, 2 or 20×10^{23} He/m^2, 900°C) on two different conditions of tungsten plate (hot rolled or recrystallized).

Generally, the results indicated little difference in the near-surface regions for the hot-rolled (HR) vs. the recrystallized (RX). However, in terms of penetration of the helium deeper (>100 nm) into the microstructure, the differences became more pronounced. Figure 3 illustrates the TEM-measured bubble structure in the four conditions; note that the first panel of the image denotes relative depths. Bubbles were binned into depths 0-50 nm, 50-100 nm, and >100 nm.

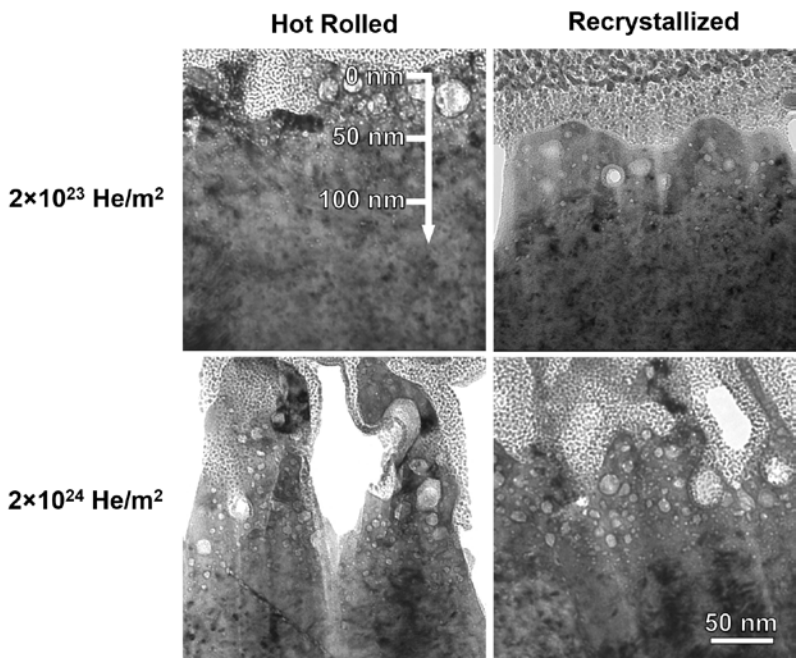

Figure 3. High-magnification TEM images showing the relative effects of microstructure and fluence. Flux ~10^{20} He/m^{2}sec, E=80 eV, T=900°C.

The differences in the distributions are shown in Figure 4. In short, the bubbles grew with fluence (which is unsurprising) but comparatively little difference was seen between the HR and RX conditions at a given depth and fluence, although at the deepest depth (>100 nm) the RX material did show the most penetration and significantly larger bubbles than in the HR material.

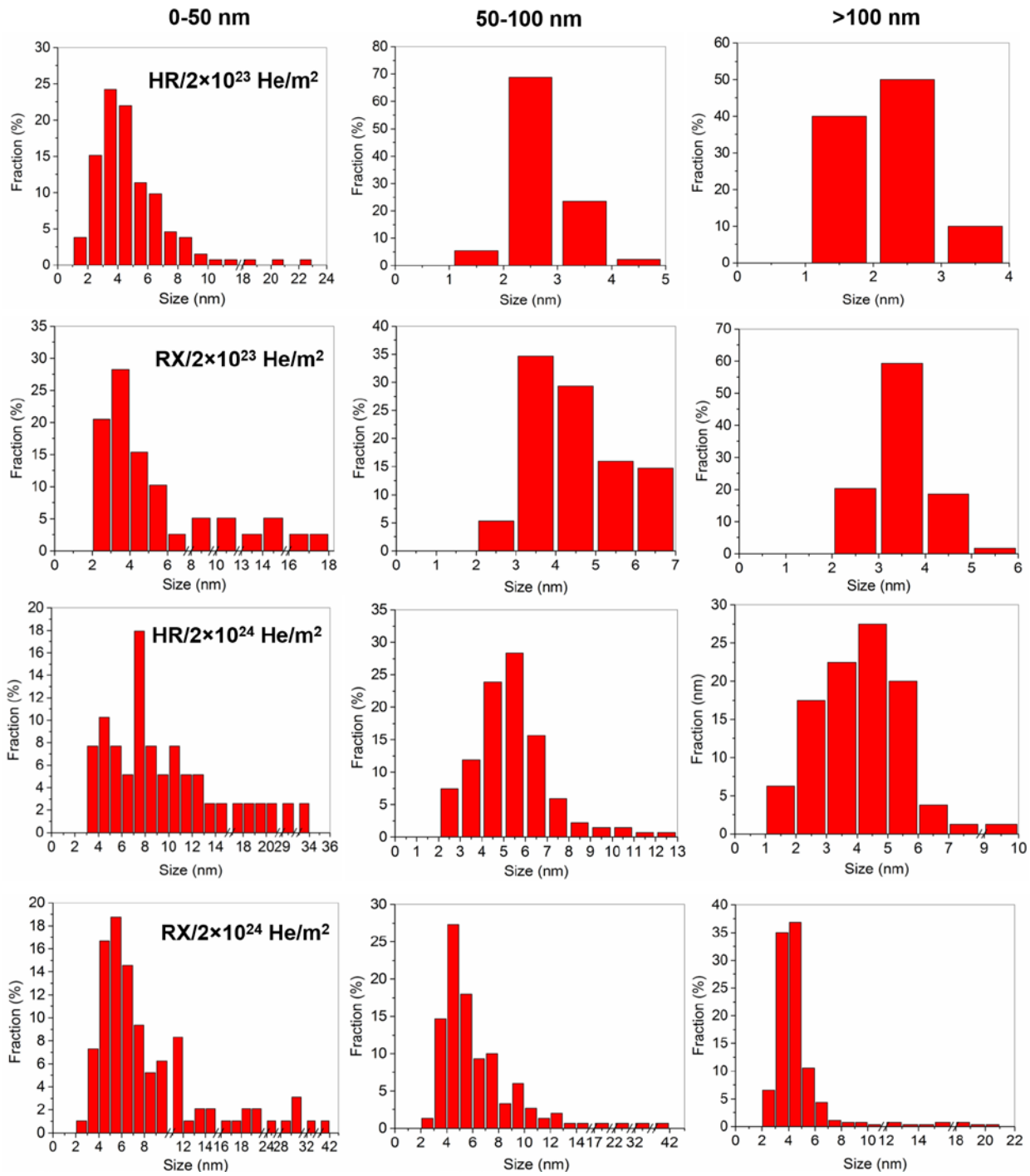

Figure 4. Size distribution of Helium cavities in various depth ranges below surface for all microstructure and fluence conditions.

Further analysis and interpretation is presently underway, but the important point to take away appears to be that at the surface, where helium concentrations will be highest, trap mutation appears to be dominant over heterogeneous nucleation on defects, which implies that materials engineering solutions at the surface to capture injected helium will require very careful consideration.

Analysis of nanotendril "fuzz"

The tKD experiments were performed on both isolated nanofuzz tendrils, and on focused ion beam (FIB) prepared specimens that contained the tendril / fuzz interface. Isolated fuzz mats or islands (Figure 5) contained small grains and many high-angle grain boundaries. Analysis of grain boundary character indicates no strong preference for any given axis/angle pair, but a slight skew toward 60° grain boundaries. Tendril grains with an obvious long axis were analyzed, and the grain long axes were also not found to have any preferred orientation.

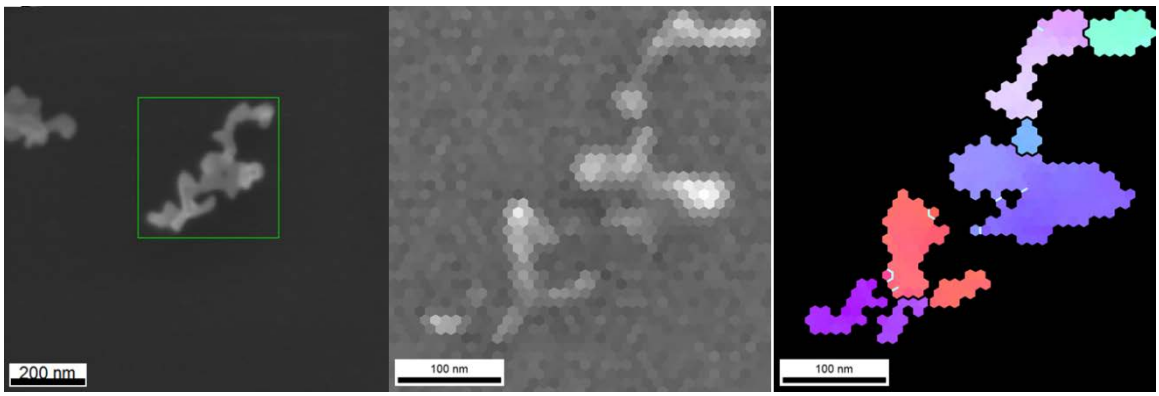

Figure 5. SEM image (left), tKD image quality map (center) and tKD grain orientation map (right) of an isolated nanotendril mat.

Examining the tendril-substrate interface is much more difficult; samples must be prepared via focused ion beam (FIB) which results in some surface damage, and more importantly, there is a slope or shank-angle to the specimens, which changes the intensity of the tKD signal and results in a concomitant baseline shift on the EBSD camera that must be accounted for; this is exacerbated at the edge of a tendril, where thickness changes rapidly. We are presently working on refining the methods, but some preliminary results have been obtained.

Figure 6 illustrates Multicharged Ion Research Facility (MIRF) exposed tungsten (HR material, 900°C, 80 eV, 20×10^{23} He/m^2), with the exact same region examined by tKD (left) and bright field TEM (right). The TEM data clearly indicates that the two tendrils are different grains than the underlying substrate; this is visible by the difference in gray scale from the substrate to the tendrils indicating a different diffracting condition. The tKD results, however, show that the rotation is actually a small angle (<15°) and therefore implies that the tendrils extending from the surface may have grown with a small rotation from the substrate, as opposed to having formed via the nucleation of an entirely new grain.

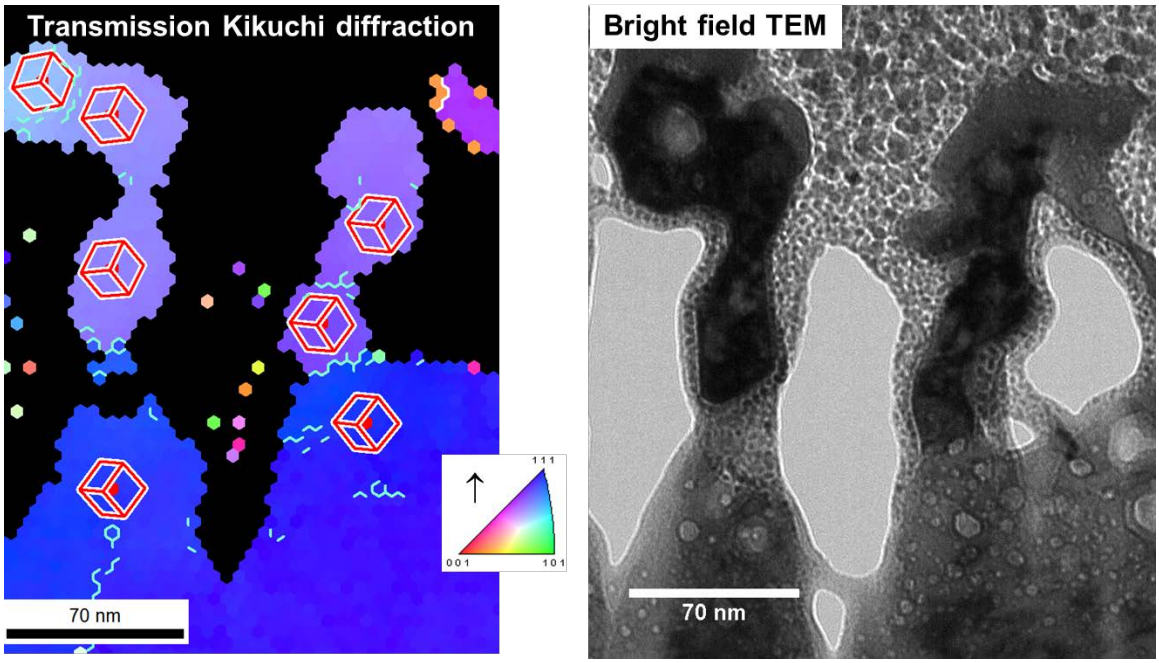

Figure 6. Left, tKD map of fuzz/substrate interface. Coloration is the IPF unit triangle projected on the vertical direction. Inset cubes are the local crystal orientation. Cyan lines are 2-15° low-angle grain boundaries. Right, BF-TEM of the same region.

Summary

We have continued to develop the necessary electron microscopy methods to examine damage mechanisms and interactions between defect types at the plasma-materials interface. We are approaching from both the near-surface plasma interactions and the neutron irradiation effects. Our goals for the next reporting period are to apply these new techniques to begin determining in detail the mechanisms underlying the specimen degradation under plasma exposure.

Acknowledgements

We thank M. Baldwin and R. Doerner, UC-San Diego, and X. Hu, F. W. Meyer and M. E. Bannister, ORNL, for collaborations. Talos F200X STEM instrument provided by the Department of Energy, Office of Nuclear Energy, Fuel Cycle R&D Program and the Nuclear Science User Facilities.